



ELSEVIER

Journal of Crystal Growth 226 (2001) 430–435

JOURNAL OF
**CRYSTAL
GROWTH**

www.elsevier.nl/locate/jcrysgr

Steady state detached solidification of water at zero gravity

Yazhen Wang, Liya L. Regel*, William R. Wilcox

International Center for Gravity Materials Science and Applications, Clarkson University, Box 5814, Potsdam, NY 13699-5814, USA

Received 14 November 2000; accepted 10 April 2001

Communicated by R.S. Feigelson

Abstract

Steady-state detached solidification of water was calculated using the Moving Meniscus Model. Similar to the experimental observation of many materials in microgravity, detached solidification of water is predicted to occur in a sealed ampoule at zero gravity under proper conditions. For steady detachment, the freezing rate must exceed a critical value, Henry's constant of the dissolved gas must be below a critical value, the temperature of the top of the water must be below a critical value, the contact angle of water on the ampoule wall must exceed a critical value, and the diffusion coefficient must exceed a critical value. Each critical value depends on the physical properties and the other operating conditions. Thus different results are obtained for InSb and water. The critical gas pressure above the melt for water is much smaller than for InSb, the critical freezing rate is larger for water, and the critical contact angle of the melt on the ampoule wall is larger for water. For the gases examined here, the solubilities of Ar, N₂ and Ne in water are sufficient for detachment to occur, while the solubility of He is not. © 2001 Elsevier Science B.V. All rights reserved.

PACS: 61.50.C; 64.70.D; 64.75; 81.10.F; 81.80

1. Introduction

Many space experiments on directional solidification have yielded ingots with sections that grew with little or no contact with the ampoule wall [1]. We call this phenomenon “detached solidification”. When detachment occurred, dislocation densities were greatly reduced and the nucleation of new grains and twins were sometimes completely eliminated. As reviewed in Ref. [2], several different types of surface features have been observed, such as isolated bubbles or voids,

hour-glass shaped necking, wavy, and meandering ridges.

Prior to the introduction of the successful Moving Meniscus Model in 1995, several mechanisms for detached solidification in microgravity had been proposed and found to be deficient [1,3]. In the Moving Meniscus Model gas dissolves in the melt and is rejected by the growing solid. A gap exists between the solid and the wall. A meniscus connects the melt at the wall with the edge of the freezing interface and moves along the ampoule wall as freezing proceeds. At steady state, the flux of gas across the meniscus and into the gap must be sufficient to maintain the pressure difference due to curvature of the meniscus.

*Corresponding author. Fax: +1-315-268-3833.

E-mail addresses: regel@clarkson.edu (L.L. Regel).

Based on the Moving Meniscus Model, numerical calculations were performed for InSb [4–7], which has frequently demonstrated detached solidification [2]. For example, we showed that when the other parameters are held constant, there is a residual gas pressure in the ampoule below which steady-state detachment cannot occur [4]. It was also shown that there is a freezing rate above which steady-state detachment does not occur [4]. The experimental observations [2] tend to show that low freezing rates favor detachment. It was predicted that detachment should occur if the growth angle exceeds a critical value, the contact angle for the melt on the ampoule wall exceeds a critical value, and the melt-gas surface tension is below a critical value [6]. For the conditions examined in Ref. [6], the sum of the growth angle and the contact angle must exceed approximately 130° in a sealed ampoule. Duffar [8] pointed out that detachment could be obtained for an ampoule open at both ends if the sum of the growth and the contact angle is sufficiently large and greater than that in a sealed ampoule.

In recent ground-based vertical Bridgman experiments, Duffar [9] imposed a gas pressure on the bottom part of the ampoule to create a meniscus between the interface and the ampoule. Detached GaSb and InSb were obtained in silica ampoules. The surface of the detached sections was similar to the results from space experiments.

Here, we determine the theoretical possibility of detachment of freezing water at zero gravity. The influence of the main operating parameters on the detachment of InSb and water was compared. In a parallel experimental study, we have been investigating the possibility of achieving detachment of ice on earth [10]. Under proper conditions, isolated gas bubbles, periodic gas tubes, and detachment with a very rough surface were obtained. It appears that microgravity experiments will be required to yield the detachment described by the steady-state Moving Meniscus Model.

2. Numerical modeling

The computer code had been developed previously [4] for steady-state detached solidification

at zero gravity. The same method was used here, as follows. First, the gap width and the parameter under investigation (e.g., the freezing rate) were assumed. The pressure inside the gap was calculated from the curvature of the meniscus and the vapor–liquid interface tension. The Navier–Stokes equations were solved to give the velocity field, which was used to calculate the concentration field of the dissolved gas. This was used to calculate the flux into the gap, and from this, a new gap width was obtained. The above process was repeated for several values of the investigated parameters. The calculated gap width was plotted versus the investigated parameter. One solution results where the calculated gap width equals the assumed gap width. A new gap width is assumed and the above process repeated to yield a plot of gap width versus the parameter under investigation.

Tables 1 and 2 show the Henry's law constant H for some gases in water used in the present calculations. Here, $X = P/H$, where P is the partial pressure of gas in torr (mm Hg) and X is the mole fraction of the gas dissolved in water at equilibrium. The other physical properties and assumed parameters for water and InSb are listed in Tables 3 and 4.

We assumed steady state, zero gravity, gap width much less than the radius R of the ampoule, no Marangoni convection (zero stress along the meniscus), slip for a short distance near the meniscus-ampoule contact line, the end of the melt far from the freezing interface, saturation of the melt with dissolved gas at the end of the melt and along the meniscus, constant average temperature of the gas in the gap, constant gap width versus

Table 1
Henry's law constant, $H \times 10^6$, for air in water at different temperatures [11]

Temperature	0°C	10°C	20°C	30°C	50°C	70°C
Air	36.3	43.7	51.6	60.2	74.2	83.5

Table 2
Henry's law constant, $H \times 10^6$, for different gases in water [11]

Gas	Ar	N ₂	Ne	He
At 0°C	16.5	32.6	76.8	100.0
At 20°C	25.8	48.6	91.4	109.0

Table 3
Relevant physical properties of InSb and water

Parameter	Symbol	Value		Reference	
		Water	InSb	Water	InSb
Vapor-melt surface tension	σ	0.000756 N/cm	0.0043 N/cm	[11]	[4]
Growth angle	α	10°	25°	[12]	[8]
Contact angle	θ	120°	112°	[13]	[4]
Kinematic viscosity	ν	$1.792 \times 10^{-3} \text{ cm}^2/\text{s}$	$3.6 \times 10^{-4} \text{ cm}^2/\text{s}$	[11]	[4]
Diffusion coefficient	D	$1.0 \times 10^{-5} \text{ cm}^2/\text{s}$	$1.0 \times 10^{-5} \text{ cm}^2/\text{s}$	[11]	[4]

Table 4

The base set of parameters used for the computations, except as noted in the results. Air was used as the base-case gas in water, with the Henry's law constants given in Table 1

Parameters	Symbol	Value	
		Water	InSb
Freezing rate	V_c	$1.5 \times 10^{-4} \text{ cm/s}$	$1.0 \times 10^{-4} \text{ cm/s}$
Average temperature of gas in the gap	T_g	273 K	800 K
Average temperature of melt at the top	T_H	293 K	830 K
Gas pressure above the melt	P_H	20 Pa	100 Pa
Segregation coefficient of dissolved gas	K	0.03	0.03

distance along the solid, and ideal gas behavior within the gap.

3. Numerical results

Refs. [4,5] show calculated velocity and concentration fields in the melt. The concentration of dissolved gas is a maximum at the center of the freezing interface, due to segregation, and is a minimum at the top of the melt. Fig. 1 shows typical results for the total flux of dissolved gas N within the melt near the meniscus, as calculated by

$$N = VC - D\nabla C \quad (1)$$

where V is the local velocity, C is the concentration of dissolved gas and D is the diffusion coefficient. The first term represents the gas carried by the motion of the fluid while the second is the flux due to diffusion. Note that here the gas flows into the meniscus near the freezing interface and out of the meniscus near the ampoule wall.

Fig. 2 compares the calculated dependence of the steady-state gap width on the gas pressure above the melt for InSb and water, with the other

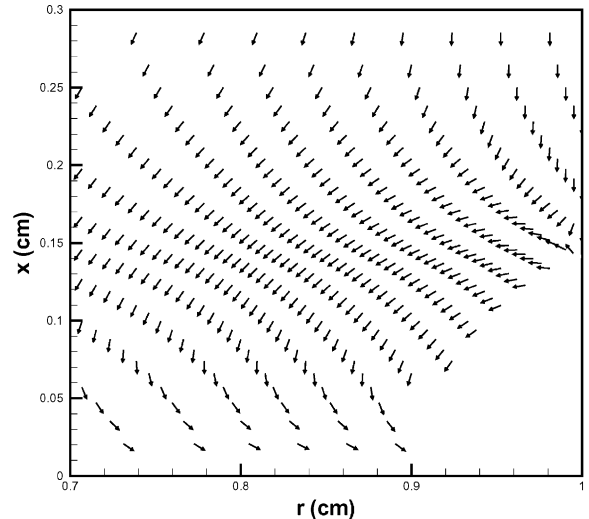


Fig. 1. Flux of dissolved gas in freezing water near the meniscus for the conditions shown in Tables 3 and 4, except with contact angle $\theta = 123^\circ$ and gap width $e = 0.1 \text{ cm}$.

parameters as given in Tables 3 and 4. Similar to InSb, in order for detachment of ice to occur, the gas pressure above the melt must be above a critical value. Note that under the assumed

conditions, the critical value for water (about 20 Pa) is much less than for InSb (about 100 Pa). From about 20–25 Pa, detachment of ice can occur with a gap from 0.01 to 0.12 cm. From about 85–120 Pa, detachment of InSb can occur with a gap from 0.01 to 0.12 cm. Above the critical value, there are two steady-state solutions, one with a large gap and one with a small gap between the solid and the wall. We do not know the extent to which both solutions can be realized in practice.

Fig. 3 compares the calculated dependence of the steady-state gap width on the freezing rate for

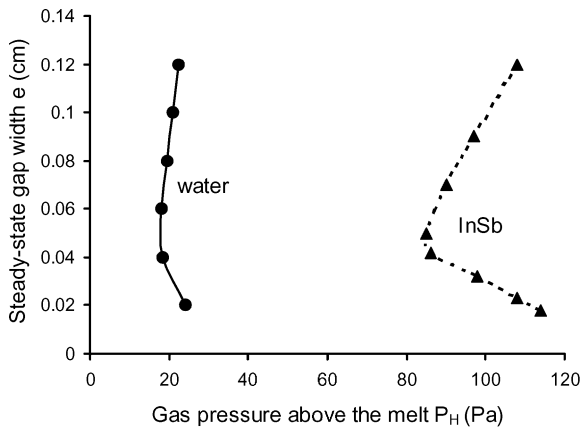


Fig. 2. The calculated dependence of the steady-state gap width e on the gas pressure above the melt P_H for water and InSb (InSb results from Ref. [4]), with the other conditions shown in Tables 3 and 4.

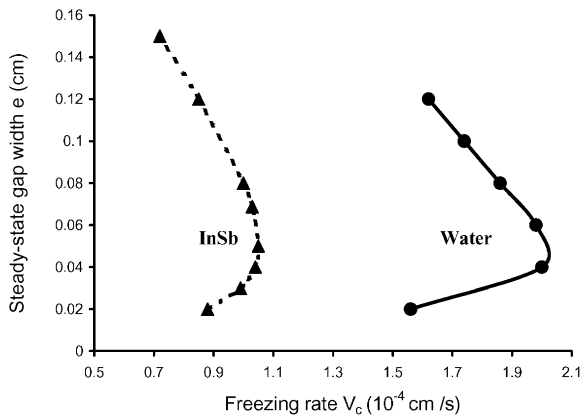


Fig. 3. The calculated dependence of the steady-state gap width on the freezing rate for water and InSb, with the other conditions shown in Tables 3 and 4.

InSb and water with the other parameters given in Tables 3 and 4. In order for detachment to occur, the freezing rate must be below a critical value.

Fig. 4 compares the calculated dependence of the steady-state gap width on the contact angle of the melt on the ampoule wall. In order for detachment of ice or InSb to occur, the contact angle should be above a critical value. In experiments, the contact angle often can be increased by coating the ampoule wall. For example, the critical value of 117° shown here for water can easily be exceeded by using a Teflon coating [13,14].

Fig. 5 shows the dependence of the gas flux into the gap on the type of gas and the gap width. Here He, Ne, N_2 and Ar were examined. At the same steady-state gap width, Ar has the largest gas flux into the gap, while He has the smallest. Fig. 6 shows the dependence of the steady-state gap width on Henry's law constant of all these gases. Here, we used the average value of H at 0°C and 20°C . In order for detachment of ice to occur, the Henry's law constant should be below a critical value (~ 87 Torr here).

Fig. 7 shows the dependence of the steady-state gap width on the temperature at the top of the water with the other conditions for air in water. In order for detachment of ice to occur, this temperature should be below a critical value (37°C here).

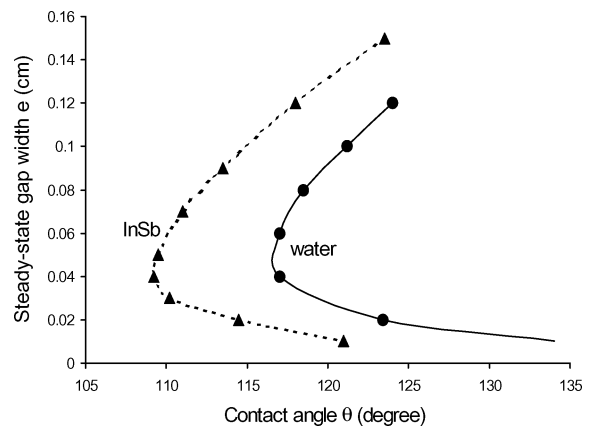


Fig. 4. The calculated dependence of the steady-state gap width on the contact angle of the melt on the ampoule wall for water and InSb [5], with the other conditions shown in Tables 3 and 4.

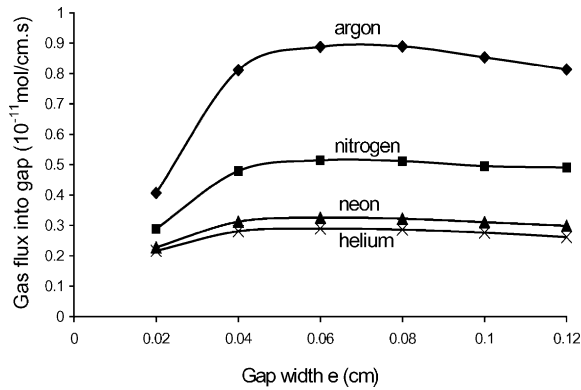


Fig. 5. The dependence of the gas flux into the gap on the gas and the gap width for water, with the other conditions shown in Tables 3 and 4.

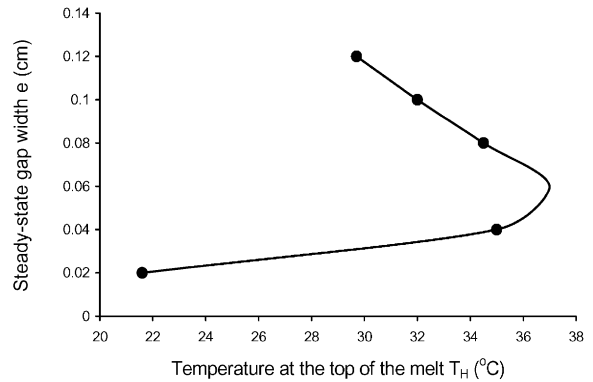


Fig. 7. The calculated dependence of the steady-state gap width on the temperature at the top of the water, with the other conditions shown in Tables 3 and 4.

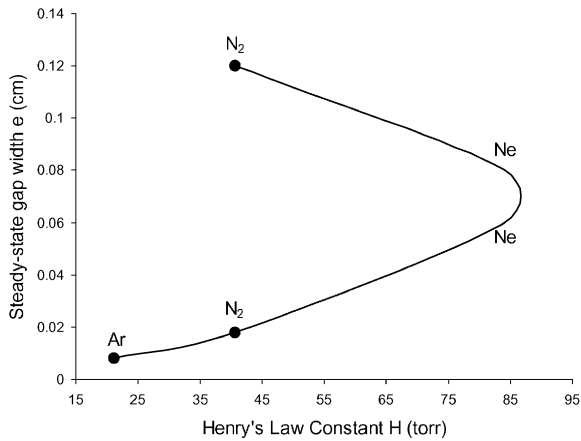


Fig. 6. The calculated dependence of the steady-state gap width on the average of Henry's constant in water at 0°C and 20°C, with the other conditions shown in Tables 3 and 4.

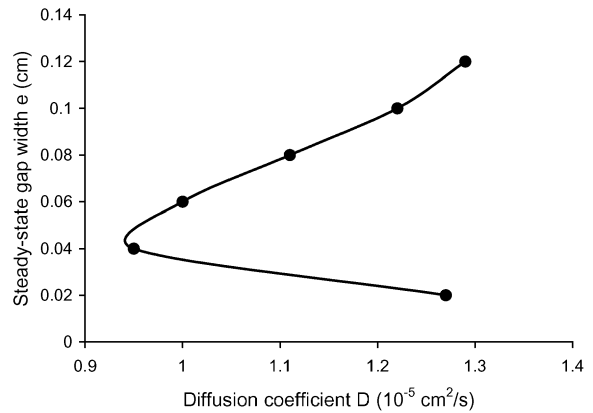


Fig. 8. The calculated dependence of the steady-state gap width on the diffusion coefficient of the dissolved gas in the water, with the other conditions shown in Tables 3 and 4.

Fig. 8 shows the dependence of the steady-state gap width on the diffusion coefficient in water. There exists a minimum value of D below which no detachment occurs.

4. Discussion

For most parameters, we obtained an extremum value for the parameter for steady-state detachment to exist, with two steady-state gap widths

that satisfied all of the equations for permissible values. This can be understood by considering the gas flux into the meniscus versus gap width or versus the parameter under consideration. The region where the dissolved gas concentration is sufficient to diffuse into the meniscus is on the order of the diffusion-layer thickness, D/V_c , where V_c is the freezing rate and D is the diffusion coefficient. Consider a very small gap width, such that the meniscus extends into the melt a distance $\ll D/V_c$. As the gap width is increased, the meniscus extends farther into the melt, and more gas diffuses in. At some gap width the conditions

for steady-state propagation are reached. With increasing gap width, the meniscus extends into the melt beyond the diffusion-layer thickness and gas diffuses out of the portion of the meniscus far from the freezing interface (as in Fig. 1). Eventually, the conditions for steady-state propagation are again reached. Similarly, for a fixed gap width decreasing the freezing rate increases the diffusion-layer thickness and leads to a maximum in total gas flux into the meniscus versus freezing rate or diffusion coefficient [4], again giving rise to two solutions to the Moving Meniscus model. We are currently investigating the stability of the two solutions with respect to perturbations.

The different physical properties of InSb and water caused a large difference in predicted behavior. The surface tension of InSb is much higher than that of water, so that the pressure difference caused by the same meniscus curvature is much larger for InSb. Thus a larger gas pressure above the melt is required for InSb to maintain the pressure balance across the meniscus. Because of the smaller growth angle for water, a larger contact angle for water is needed to obtain a given meniscus curvature. The different growth angles, contact angles and surface tensions caused the differences in critical freezing rates.

The higher the Henry's law constant (Table 2), the smaller the solubility of gas for the same gas pressure. In order for detachment to occur, the gas concentration in the melt must exceed a critical value. When Henry's law constant for a gas in water is higher than a critical value, the solubility of the gas is not enough for detachment of ice to occur. So under the conditions examined here, detachment should not occur with He, and should be possible for Ar, N₂ and Ne.

The temperature at the top of the melt affects the temperature gradient of the melt near the interface, and thereby the variation in solubility along the meniscus. The solubility of air in water decreases as temperature increases, as shown in Table 1. When the temperature at the top of the water is higher than a critical value, the amount of air dissolved in water is too small for sufficient gas

to diffuse into the gap for detachment to occur. So the temperature T_h at the top of the water should be below a critical value. Consistent results were observed in our recent experiments on freezing of water [10]. Gas bubbles and tubes grew on the ampoule wall only when the hot zone temperature was below a critical value.

Acknowledgements

This research was supported by NASA grant NAG 8-1482. We are grateful to NASA's Marshall Space Flight Center for use of their supercomputer.

References

- [1] W.R. Wilcox, L.L. Regel, *Microgravity Sci. Technol.* 8 (1995) 56.
- [2] L.L. Regel, W.R. Wilcox, *Microgravity Sci. Technol.* 11 (1999) 152.
- [3] L.L. Regel, W. R. Wilcox, *Proceedings of the First Pan-Pacific Basin Workshop and Fourth Japan–China Workshop on Microgravity Sciences*, *J. Jpn. Soc. Microgravity Appl.* 15 (1998) 460.
- [4] D.I. Popov, L.L. Regel, W.R. Wilcox, *J. Mater. Synth. & Proc.* 5 (1997) 283.
- [5] Y. Wang, L.L. Regel, W.R. Wilcox, *J. Crystal Growth* 209 (2000) 175.
- [6] D.I. Popov, L.L. Regel, W.R. Wilcox, *J. Mater. Synth. & Proc.* 5 (1997) 299.
- [7] D.I. Popov, L.L. Regel, W.R. Wilcox, *J. Mater. Synth. & Proc.* 5 (1997) 313.
- [8] T. Duffar, I. Paret-Harter, P. Dusserre, *J. Crystal Growth* 100 (1991) 171.
- [9] T. Duffar, P. Dusserre, F. Picca, S. Lacroix, N. Giacomtti, *J. Crystal Growth* 2 (2000) 434.
- [10] Y. Wang, L.L. Regel, W.R. Wilcox, *The formation and growth of gas bubbles and tubes by freezing water using the VBS technique*, submitted for publication.
- [11] D.R. Lide (Ed.), *Handbook of Chemistry and Physics*, 76th edition, 1995–1996, Chemical Rubber Publishing Company, 2000 Corporate Blvd., N.W., Boca Raton, Florida 33431.
- [12] G.N. Milshchev, *Bulgarska Akademiia na Naukite, Sofia Doklady* 26 (1973) 1335.
- [13] C. Burkhard, L.L. Regel, W.R. Wilcox, *High contact-angle coatings for glass*, submitted for publication.
- [14] C. Burkhard, M.S. Thesis, Clarkson University, 2001.